2024 IEEE International Symposium on Biomedical Imaging (ISBI) | 979-8-3503-1333-8/24/$31.00 ©2024 IEEE | DOI: 10.1109/ISBI56570.2024.10635174

LEARNING BREAST TISSUE PRONE-TO-SUPINE DISPLACEMENT FOR SURGICAL PLANNING WITH CONVOLUTIONAL NEURAL NETWORKS

F. Alfano[1,2], *D. Bermejo-Pelaez*[3,1,2], *L. Cordero-Grande*[1,2], *K. Ferreres Garcia*[4], *J.E. Ortuño Fisac*[2,1], *O. Bueno Zamora*[4], *S. Lizarraga*[4], *A. Santos*[1,2], *J. Pascau*[5], *M.J. Ledesma-Carbayo*[1,2]

[1] Biomedical Image Technologies, Universidad Politécnica de Madrid. Madrid, España
[2] CIBER-BBN, ISCIII, Madrid, España [3] Spotlab, Madrid, España [4] Instituto de Investigación Sanitaria Gregorio Marañón. Madrid, España [5] Departamento de Bioingeniería, Universidad Carlos III de Madrid. Madrid, España

ABSTRACT

Breast-conserving surgery is the preferred treatment for non-palpable early-stage breast tumors. MRI images in the prone position are commonly used for accurate diagnosis of lesions. However, as the procedure is performed in the supine position, significant breast deformation occurs. Therefore, preoperative localization of the lesions is necessary to ensure their effective removal during surgery. In this study, we propose a novel deep learning based approach to predict the large deformation of the preoperative volume of the breast given the intraoperative surface. We use a fully connected network trained in a supervised manner using synthetic generated ground-truth displacement vector fields. We evaluated the method in 10 real clinical cases with an average tumor localization error of 15.46 ± 3.96 mm and an average tumor-skin projection distance of 13.38 ± 4.61 mm.

***Index Terms*—** Breast cancer, Surgical planning, Surface-to-volume registration

1. INTRODUCTION

Breast conserving surgery (BSC) is the preferred therapeutic approach for non-palpable early-stage breast cancers. Despite the effectiveness of preoperative MRI images in accurately identifying the location of lesions, their utility for surgical planning is limited because MRI is conducted in the prone position, while the surgery takes place in the supine position. AS the breast undergoes significant deformation when shifting from the prone-to-supine positions, preoperative localization techniques are required to target the lesion and ensure their precise surgical removal.

Wire-guided localization (WGL) is currently the most commonly used method for locating non-palpable breast lesions [1]. However, this technique has limitations, including technical challenges like wire transection and migration, patient discomfort, and suboptimal cosmetic results [2], [3]. Due to the current limitations of intraoperative tumor localization approaches, several groups have investigated alternative approaches based on medical imaging data to support surgical planning or guidance [4].

Typically, these proposals rely on biomechanical simulations alone [5]–[7] or integrate biomechanical simulation with intensity-based image registration when a supine MRI or CT is available [8]–[10]. Other groups have proposed the use of the intraoperative surface data obtained from optical scans or other supine imaging to predict the deformation of the preoperative MRI volumes. Typically, these methods involve finite element method (FEM) models with boundary conditions derived from intraoperative data [11]–[13], and some also incorporate image registration techniques [10].

Previous studies have investigated real-time intraoperative organ deformation using deep learning (DL). These methods integrate preoperative volume information and intraoperative partial surface data to facilitate real-time surgical guidance and navigation. Such methods can learn the intrinsic biomechanical model, allowing for accurate predictions at haptic feedback rates. Pfeiffer et al. [14] developed a neural network for predicting displacement fields exclusively using synthetic data generated from random organ-like meshes. The aim was to estimate displacement fields within a liver, with the input being the surface displacement. Mendizabal et al. [15] proposed a neural network capable of predicting the deformation of an elastic structure in response to varying external forces or surface deformations. Their application of this method included real-time tracking of breast lesions during ultrasound-guided breast biopsy, using a breast phantom for experimentation [16]. The main limitations of these physics-based learning methods are related to the data generation process. The number of simulations required to train the network is very time consuming and increased grid resolution requires longer training time. Additionally, this approach is patient-specific and requires offline FEM-based data generation for each different geometry.

In this work, we propose a new approach that combines DL-based image and shape registration techniques to predict the large deformation of the preoperative volume of the breast given the intraoperative surface. Our method is geometry-independent and uses signed distance field (SDF) images for encoding both the preoperative volume and intraoperative surface. We use a fully connected network trained in a supervised manner using as ground-truth displacement vector fields (DVFs) generated through a landmark driven LDDMM registration method that relies on external and internal correspondences. Moreover, different loss metrics have been proposed, one emphasizing only global deformation and another considering also the surface and the internal structures. The method is very efficient and applicable in the intraoperative context.

2. METHODS

The goal of the work presented in this chapter is to estimate the displacement of the breast and the tumor when given a) the preoperative geometric model of the breast extracted from a preoperative prone image and b) the surface of the intraoperative surface as could be acquired by an intraoperative optical scan. Figure 1 shows a graphical representation of the proposed approach, aiming to train a network

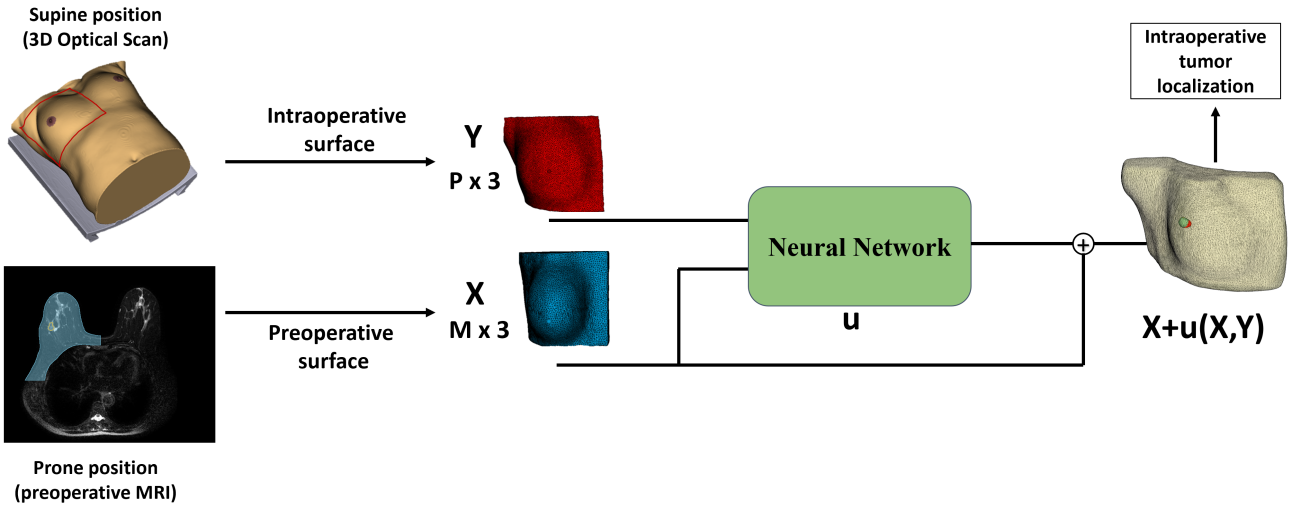

Fig. 1. Method overview: given preoperative and intraoperative surfaces as inputs the goal is to train a network capable of accurately determining breast tumor deformation and tumor localization in the surgical setting.

capable of accurately determining tumor localization with preoperative and intraoperative surfaces as inputs.

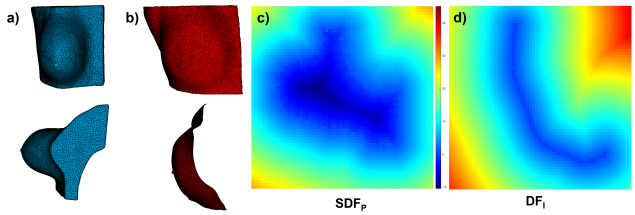

Fig. 2. a) Preoperative volume mesh V_P. b) Intraoperative surface S_I. c) Signed distance field of preoperative volume SDF_P (axial view). d) Distance field of the intraoperative surface DF_I (axial view).

2.1. Voxelization

To overcome the inconsistency of the input dimensionality we converted the points sets into a regular grid representation. Thus, the input of the network is a cube of voxels, and the output of the network becomes a displacement field with a three-dimensional displacement vector for each of these voxels. Unlike other methods that use a voxel-grid representation of the point cloud or the mesh [15], [17] we found that encoding the preoperative and intraoperative input meshes using a voxelization in the form of distance fields on a regular grid significantly improves efficiency and convergence. To obtain the distance field representation of the preoperative volume V_P we calculated the distance of each point of the grid p to the closest surface point of the preoperative volume and flipped the sign of the grid points enclosed in the surface of the preoperative volume resulting in a signed distance field SDF_P. Similarly, the distance field for the open intraoperative mesh DF_I was obtained using the same procedure, with the distinction that it does not include negative values due to the open nature of this mesh. SDF_P and DF_I are shown in Figure 2.c and 2.d. If we denote by $\mathbf{X}$ all points of the preoperative volume V_P and $\mathbf{Y}$ the points of the intraoperative surface S_I, the goal is to find a displacement function (a vector field) $u : \mathbb{R}^{M\times 3} \times \mathbb{R}^{P\times 3} \rightarrow \mathbb{R}^{M\times 3}$ such that $\mathbf{Y} + u(\mathbf{Y}, \mathbf{X})$ matches $\mathbf{X}$ as closely as possible. Where M and P are the numbers of points of X and Y respectively. We sample the cubical volume into a grid G of $64 \times 64 \times 64$ points of interest.

2.2. Ground-truth Generation

Figure 3 reports the workflow for the generation of ground-truth displacement vector fields (DVFs) used as reference to train the network (U_{GT}). Following an initial rigid alignment, we establish a set of surface fiducial points based on the nipple position. These points serve to track correspondences between the prone and supine surfaces. The whole surface to surface correspondence is obtained using a Laplacian Surface Deformation followed by an ICP algorithm. The resulting surface and the tumor points correspondences guide a Landmark-Driven Deformable Registration (LDDMM) algorithm, producing displacement vectors for all points in the preoperative breast volume and transforms the prone volume into the supine configuration. Utilizing a landmark-driven LDDMM algorithm ensures distance minimization between landmarks, while preserving volume, ensuring smoothness of displacement vector fields, and maintaining consistency. Detailed information of the methodology for the estimation of tumor position is available in [18]. In this case we have added the information on the real tumor position to generate the best possible ground truth. To obtain a reliable ground-truth DVF we have optimized the parameters of the LDDMM algorithm until the LDDMM-estimated positions of the nipple and tumor centroid satisfied a predefined distance requirement ($< 3.5\ mm$ for the tumor centroid and $< 6\ mm$ for the nipple).

2.3. Network Architecture and Training

In order to estimate the displacement field U_{EST}, the network is given the full preoperative prone volume SDF_P and the intraoperative surface DF_I. Before feeding the data to the network, we normalize SDF_P, DF_I to improve the convergence properties. Formally, we want the network to estimate the function:

$$F(SDF_P, DF_I) = U_{EST} \tag{1}$$

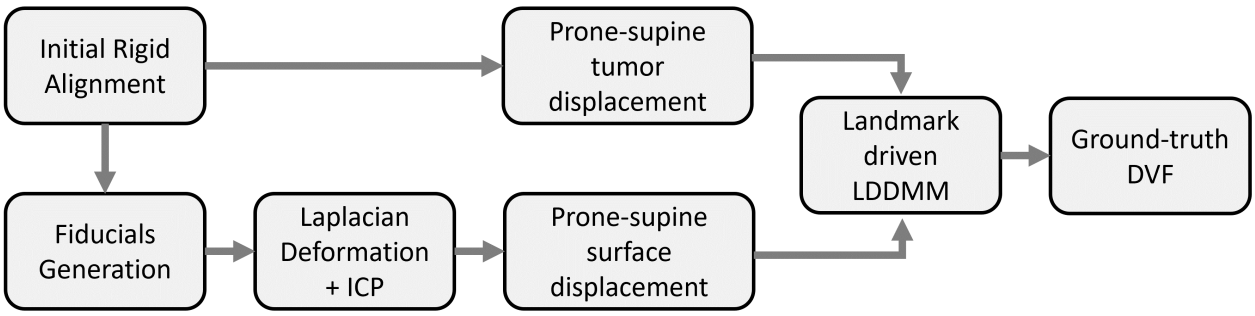

Fig. 3. Workflow for the generation of ground-truth DVFs used as reference to train the network (based on [18]).

We employ DispVoxNet network D_{vn} as our base architecture, following the design proposed by Shimada et al. [17]. Featuring an encoder-decoder structure and skip connections, it enables abstract low-resolution representation while preserving high-resolution details. Unlike the original U-Net [19], our network operates with three-dimensional input data and the loss and the output is related to the estimation of the desired displacement field. Each convolution has a kernel side length of 3, padding of 1, and is succeeded by a LeakyReLU activation function. We refer to our D_{vn} modified architecture that includes SDF images as D_{vn-SDF}.

The displacement field output from the network U_{EST} is compared to the ground-truth displacement field U_{GT} using the mean absolute error. U_{GT} is also normalized to enhance convergence.

Given a grid G of $N \times N \times N$, the loss function L_{MSE}, that calculates the mean squared error (MSE), is written as follows:

$$L_{MSE} = \frac{1}{N^3} \sum_{p} M(p) \parallel U_{EST}(p) - U_{GT}(p) \parallel \qquad (2)$$

where N^3 is the number of points of the grid, $M(p)$ is a masking function that is 0 if p is outside the prone breast volume and 1 otherwise and $\parallel \bullet \parallel$ denotes the magnitude of a vector.

We also designed another loss function:

$$L_{ST} = \alpha L_{MSE} + \beta L_S + \gamma L_T \qquad (3)$$

Where L_S is defined as the mean of the smallest distances of every point p_{SP} of the preoperative surface S_P to any points p_{SI} of the intraoperative surface S_I:

$$L_S = \frac{1}{N_{SP}} \sum_{p_{SP} \in S_P} \{ \min_{p_{SI} \in S_I} \{ d(p_{SP}, p_{SI}) \} \} \qquad (4)$$

L_T is defined as the mean of the smallest distances of every points p_{TP} of the preoperative tumor T_P to any point p_{TI} of the intraoperative tumor T_I:

$$L_T = \frac{1}{N_{TP}} \sum_{p_{TP} \in T_P} \{ \min_{p_{TI} \in T_I} \{ d(p_{TP}, p_{TI}) \} \} \qquad (5)$$

N_{SP} and N_{TP} denote the number of points of the preoperative surface S_P and tumor T_P, respectively.

We experimentally fixed the weights values in (3) to $\alpha = 10$, $\beta = 0.5$, $\gamma = 1$. Adding these terms to the computation of the loss allows to specifically penalize the distance between the deformed preoperative and intraoperative surfaces, and the distance between the estimated and real tumor.

We trained the network with Adam optimizer [20] with a learning rate of $3 \cdot 10^{-4}$. Furthermore, we used a 5-fold cross-validation with 1500 epochs, and selected the model with the best convergence of the mean registration error.

3. EXPERIMENTS AND RESULTS

Dataset comprised 69 retrospective cases of breast cancer, each including a preoperative T2 SPAIR MRI and a CT image in the supine position used to simulate the intraoperative surface and to locate the tumor in the supine position for evaluation assessment. Table 1 reports the range and average value of a set of descriptive variables of the dataset including breast volume, tumor extension, and total tumor displacement from the prone to supine position of the samples.

	Range	**Mean**
Age [years]	32 - 87	63
Breast volume [cm^3]	812.8 - 4359.2	1948.3
Tumor diameter [mm]	4.5 - 33,6	15.7
Tumor-skin distance [mm]	5.3 - 45.7	21.6
Prone-to-supine tumor displacement [mm]	23.6 - 180.4	71.7

Table 1. Patients and Tumor Characteristics.

The augmentation of cases considered both the tumor-affected breast and the contralateral breast, which can vary in shape and constitution, leading to different deformations. Therefore, the final number of breasts in the dataset was 138. In the case of controlateral breast samples, we assumed $\gamma = 0$ in the computation of the loss L_{ST} (see eq. (3). We used 118 breasts for training and the remaining for testing, ensuring an equal distribution of breast sizes between the two sets. Moreover, the partitioning guaranteed that complete cases, comprising the tumor-affected breast and its corresponding contralateral breast, were exclusively assigned to either the training or testing sets. Consequently, 10 cases were used for the estimation of tumor-related metrics.

We conducted experiments with two network models of D_{vn-SDF}, each trained with the loss L_{MSE} and L_{ST}. The same data partitioning was applied in both experimental setups.

The network was implemented using PyTorch [21], and built in a PC with a GPU NVIDIA GeForce GTX 1080 8GB and NVIDIA Quadro P6000 24GB.

We assessed the registration accuracy using the distance between the estimated and actual tumor centroids and the distance between the skin projections of the estimated and actual tumor centroids.

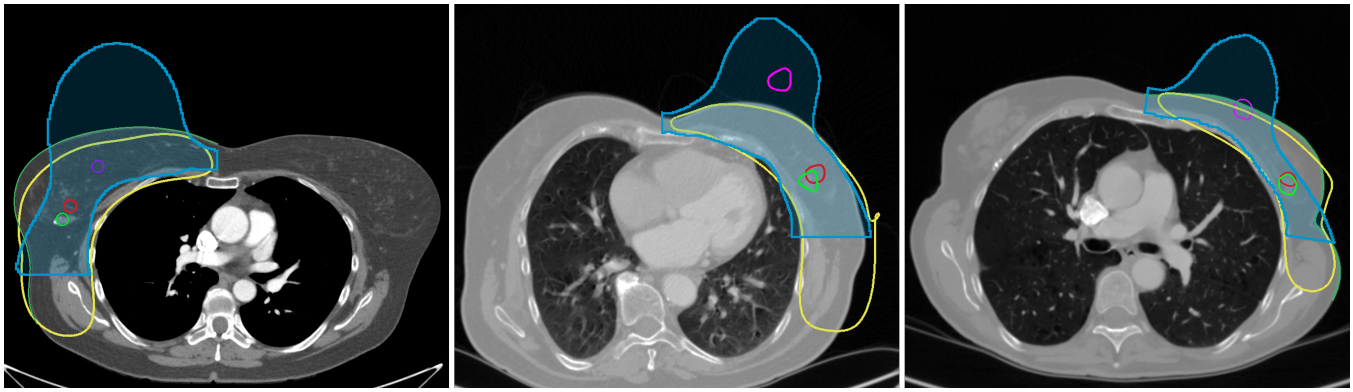

Fig. 4. Result of the D_{vn-SDF} - L_{ST} model in three different cases. The blue region denotes the preoperative breast volume, with the magenta line indicating the preoperative tumor. The yellow line outlines the estimated deformed mesh, while the green and red lines represent the actual and estimated tumors, respectively.

Model	Tumor Distance [mm]	Skin projection Distance [mm]
D_{vn-SDF} - L_{MSE}	17.40 ± 6.10	14.71 ± 6.21
D_{vn-SDF} - L_{ST}	15.46 ± 3.96	13.38 ± 4.61
Landmark driven LDDMM	16.52 ± 6.82	15.05 ± 6.68

Table 2. Results obtained with D_{vn-SDF} - L_{MSE}, D_{vn-SDF} - L_{ST} and the Landmark driven LDDMM registration framework.

Table 2 displays the comparison of the results obtained by the model D_{vn-SDF} trained with the losses L_{MSE} and L_{ST}. Figure 4 shows the qualitative results obtained from the D_{vn-SDF} - L_{ST} model, which demonstrated superior performance. Table 2 also shows the results comparison with the original landmark driven LDDMM registration algorithm [18].

Given a preoperative volume and an intraoperative surface encoded in a distance field image, the prediction of the displacement field with the $D_{vn-SDF} - L_{ST}$ model takes approximately 130 ms. This marks a significant improvement compared to the original D_{vn} model, which relies on a voxelized version of input surfaces and demands significantly longer training and inference times (more than an order of magnitude in comparison to our proposed approach).

The LDDMM based alternative method took around 2 minutes per inference, which it is also substantially improved. Moreover, precision is improved as tumor mean distances and their variability in the test cases decreased.

4. DISCUSSION AND CONCLUSIONS

In this study, we developed a novel DL-based approach to effectively model substantial prone-to-supine breast deformation and predict intraoperative tumor position, aiding in surgical planning for breast cancer treatment. We adapted the architecture proposed by [17], designed for point-sets alignment and trained with thousand of meshes with known ground-truth displacement vectors, to be used for a surface to volume registration. Furthermore, we adopted a distance field representation of the inputs that was more efficient and allowed faster training and prediction. The network was trained in a supervised manner using as ground-truth displacement vector fields generated with a landmark driven LDDMM registration method that rely on external and internal correspondences. Additionally, different loss metrics were designed and compared: L_{MSE}, focusing solely on global deformation and L_{ST} that also takes into account the surface and the tumor structures.

The method was evaluated in 10 real clinical cases. Better results were obtained using the D_{vn-SDF} - L_{ST} model with an average tumor localization error of 15.46 ± 3.96 mm and an average surface projection distance of 13.38 ± 4.61 mm.

The model performance (see Table 2) is comparable to the landmark driven registration framework proposed in our previous publication [18]. However, in this current approach, the results are more precise and the prediction of the displacement field requires approximately 130 ms, a substantial improvement compared to the alternative method which took around 2 minutes. Other state-of-the-art DL-based registration methods use images as inputs and rely on image similarity metrics. Therefore, a comparison with these methods was not feasible [22]–[24].

Some comparable methods, based only on surgical surface data, produced similar results (average landmarks distance of 15.3 mm in 3 cases [12]) or worse results (average tumor-skin projection distance of 20.8 mm in 9 cases [13]). No information is given in these works about the distribution of breast sizes.

Due to the high speed, this method could also be used in other real-time applications in surgery or radiation therapy. Furthermore, it could be used as an initial fast alignment before other registration techniques. The network can be easily used with different breast geometries that have not been seen during training, in contrast to other proposals that need a new training for every new geometry [15]. Furthermore, our method has been tested in 10 clinical cases, unlike other similar proposals [14] with less validation cases.

In conclusion, we have developed a method that, relying solely on intraoperative surface data, shows a high ability to recover large breast deformations and competitive results in terms of tumor localization accuracy. Moreover, the associated computation times are fully compatible with real-time applications in surgical setting. This study provides evidence of the ability of DL methods to estimate large deformations in real time in different organ models distinct from those used during their training. This highlights the innovative potential of our proposal across various clinical applications.

5. COMPLIANCE WITH ETHICAL STANDARDS

This research study was conducted using retrospective data and it was approved by the institutional review board from Hospital Gregorio Marañón.

6. ACKNOWLEDGMENTS

The authors acknowledge the support of Ministerio de Ciencia e Innovación, Agencia Estatal de Investigación, under grants PDC2022-133865-I00 and PID2022-141493OB-I00, TED2021-129392B-I00 (MCIN/AEI/10.13039/501100011033) and Project PI18/01625 (Instituto de Salud Carlos III), co-financed by European Regional Development Fund (ERDF), 'A way of making Europe' and 'NextGenerationEU'/PRTR.

References

[1] B. K. Chan *et al.*, "Localization techniques for guided surgical excision of non-palpable breast lesions," *Cochrane Database of Systematic Reviews*, no. 12, 2015.

[2] J. H. Volders *et al.*, "Current status of ultrasound-guided surgery in the treatment of breast cancer," *World journal of clinical oncology*, vol. 7, no. 1, p. 44, 2016.

[3] N. Kiruparan *et al.*, "Use of wire guided localisation and radio-guided occult lesion localisation for non-palpable breast lesions: A systematic literature review and meta-analysis of current evidence," *Asian Journal of Surgery*, 2021.

[4] J. H. Hipwell *et al.*, "A review of biomechanically informed breast image registration," *Physics in Medicine and Biology*, vol. 61, no. 2, R1–R31, Jan. 2016.

[5] A. P. del Palomar *et al.*, "A finite element model to accurately predict real deformations of the breast," *Medical Engineering & Physics*, vol. 30, no. 9, pp. 1089–1097, Nov. 2008.

[6] V. Vavourakis *et al.*, "Multiscale mechano-biological finite element modelling of oncoplastic breast surgery —numerical study towards surgical planning and cosmetic outcome prediction," *PloS one*, vol. 11, no. 7, e0159766, 2016.

[7] T. P. Babarenda Gamage *et al.*, "An automated computational biomechanics workflow for improving breast cancer diagnosis and treatment," *Interface Focus*, vol. 9, no. 4, p. 20 190 034, Aug. 2019.

[8] T. Carter *et al.*, "Mr navigated breast surgery: Method and initial clinical experience," in *International Conference on Medical Image Computing and Computer-Assisted Intervention*, Springer, 2008, pp. 356–363.

[9] L. Han *et al.*, "A nonlinear biomechanical model based registration method for aligning prone and supine mr breast images," *IEEE transactions on medical imaging*, vol. 33, no. 3, pp. 682–694, 2013.

[10] C. Xue *et al.*, "Multimodal patient-specific registration for breast imaging using biomechanical modeling with reference to ai evaluation of breast tumor change," *Life*, vol. 11, no. 8, p. 747, 2021.

[11] M. A. Lago *et al.*, "Breast prone-to-supine deformation and registration using a Time-of-Flight camera," in *2012 4th IEEE RAS EMBS International Conference on Biomedical Robotics and Biomechatronics (BioRob)*, ISSN: 2155-1782, Jun. 2012, pp. 1161–1163.

[12] B. Eiben *et al.*, "Surface driven biomechanical breast image registration," in *Medical Imaging 2016: Image-Guided Procedures, Robotic Interventions, and Modeling*, SPIE, vol. 9786, 2016, pp. 282–291.

[13] M. Duraes *et al.*, "Surgery of nonpalpable breast cancer: First step to a virtual per-operative localization? First step to virtual breast cancer localization," *The Breast Journal*, vol. 25, no. 5, pp. 874–879, Sep. 2019.

[14] M. Pfeiffer *et al.*, "Non-rigid volume to surface registration using a data-driven biomechanical model," in *International Conference on Medical Image Computing and Computer-Assisted Intervention*, Springer, 2020, pp. 724–734.

[15] A. Mendizabal *et al.*, "Simulation of hyperelastic materials in real-time using deep learning," *Medical Image Analysis*, vol. 59, p. 101 569, Jan. 2020.

[16] A. Mendizabal *et al.*, "Physics-based deep neural network for real-time lesion tracking in ultrasound-guided breast biopsy," in *Computational Biomechanics for Medicine*, K. Miller *et al.*, Eds., Cham: Springer International Publishing, 2020, pp. 33–45.

[17] S. Shimada *et al.*, "DispVoxNets: Non-Rigid Point Set Alignment with Supervised Learning Proxies," in *2019 International Conference on 3D Vision (3DV)*, Québec City, QC, Canada: IEEE, Sep. 2019, pp. 27–36.

[18] F. Alfano *et al.*, "Breast tumor localization by prone to supine landmark driven registration for surgical planning," *IEEE Access*, vol. 10, pp. 122 901–122 911, 2022.

[19] O. Ronneberger *et al.*, "U-net: Convolutional networks for biomedical image segmentation," in *International Conference on Medical image computing and computer-assisted intervention*, Springer, 2015, pp. 234–241.

[20] D. P. Kingma *et al.*, "Adam: A method for stochastic optimization," *arXiv preprint arXiv:1412.6980*, 2014.

[21] A. Paszke *et al.*, "Pytorch: An imperative style, high-performance deep learning library," *Advances in neural information processing systems*, vol. 32, 2019.

[22] G. Balakrishnan *et al.*, "Voxelmorph: A learning framework for deformable medical image registration," *IEEE transactions on medical imaging*, vol. 38, no. 8, pp. 1788–1800, 2019.

[23] B. Kim *et al.*, "Cyclemorph: Cycle consistent unsupervised deformable image registration," *Medical image analysis*, vol. 71, p. 102 036, 2021.

[24] M. Kang *et al.*, "Dual-stream pyramid registration network," *Medical image analysis*, vol. 78, p. 102 379, 2022.